Available online at www.sciencedirect.com
ScienceDirect
Trans. Nonferrous Met. Soc. China 25(2015) 2137−2146
Transactions of Nonferrous Metals Society of China
www.tnmsc.cn

Microstructure characterization and mechanical properties of gas tungsten arc welded cast A356 alloy

S. TAKHTI, M. REIHANIAN, A. ASHRAFI

Department of Materials Science and Engineering, Faculty of Engineering, Shahid Chamran University of Ahvaz, Ahvaz 61357−83151, Iran

Received 13 August 2014; accepted 13 March 2015

Abstract: The microstructure and mechanical properties of the gas tungsten arc welded cast A356 alloy were investigated with fillers ER1100, ER4043, ER4047 and ER5356 under the pulse frequencies of 1, 3 and 5 Hz. Results showed that the filler metal and pulse frequency affected the grain structure of fusion zone considerably. The highest fraction of eutectic (44%) was formed with filler ER4047. Tensile fracture of all specimens indicated that fracture did not occur in the fusion zone. The greatest impact toughness (about 4 J) was achieved for the welds with filler ER4047 while the largest hardness (HV 90) was obtained with filler ER5356.
Key words: cast A356 alloy; gas tungsten arc welding; microstructure; hardness; impact energy

1 Introduction

Cast A356 Al alloys have widespread applications in general engineering applications, particularly in the automotive and aerospace industries. This is due to their outstanding castability, corrosion resistance and high specific strength. Cast A356 alloy is an Al−Si−Mg system whose basic alloying elements are Si (6.5%−7%, mass fraction) and Mg (0.2%−0.4%, mass fraction). The effects of silicon are the enhancement of casting characteristics and improvement of the fluidity, hot crack resistance and feeding characteristics of the cast alloy. In addition, Mg causes the increase in the specific strength, which is the basis for mechanical properties of the alloy.

Many industrial purposes imply that Al castings need to be welded to themselves or to the wrought alloys. To date, many works have been focused on investigating the welding characteristics of the wrought Al−Si−Mg alloys [1−6]. Among the many welding techniques, friction stir welding is the most common method for welding of the cast A356 alloy to itself or to other Al alloys [7−11]. Nevertheless, only slight attempts have been made for welding of the cast A356 alloys by laser welding [12, 13] and gas tungsten arc (GTA) welding [14,15].

HWANG et al [14] investigated the effect of welding parameters on the quality of the GTA welded A356 alloy. A squeeze-cast A356 alloy was used as their initial material. They reported that squeeze casting, which is a combination of casting and forging processes, is beneficial for poor castability alloys and displays good mechanical properties. Their results indicated that a great amount of porosity is formed in the fusion zone of the squeeze cast A356 alloy before T6 heat treatment. In addition, filler Al−5Mg significantly decreased the number of pores compared to the welds with filler Al−5Si. RATNAKUMAR and SRINIVASA RAO [15] studied the corrosion behavior of the weld metal, partially melted zones and heat-affected zones of GTA welds in A356 alloy with different prior thermal tempers. They used the continuous and pulsed current GTA welding techniques and showed that the partially melted zone of the welds was attacked severely. They found that pulsing technique could decrease the severity of corrosion in the partially melted zone. In addition, they found that the prior thermal condition influenced the corrosion of heat- affected zones of welds.

Apart from the mentioned previous works, the welding characteristic of the cast A356 Al alloy has been rarely reported and still needs further investigation. Accordingly, in the present work, GTA welding was used

Corresponding author: M. REIHANIAN; Tel: +98-61-3333001019-5684; Fax: +98-61-33336642; E-mail: reihanian@scu.ac.ir
DOI: 10.1016/S1003-6326(15)63825-0

for joining of the cast A356 alloy. A356 alloy was made by sand casting method. The effects of filler metal and welding frequency on the microstructure and mechanical properties of the weld bead were examined.

2 Experimental

A356 alloy was cast by sand casting method. The molten alloy was modified by strontium (Sr) to control the size and morphology of eutectic silicon and improve the properties of the alloy. The as-cast ingots were machined into rectangular plates of 100 mm × 50 mm × 5 mm. A pulsed current GTA welding machine was used in this work. The A356 Al alloy plate was joined through single-pass welding. Based on the capacity of welding machine, three pulse frequencies of 1, 3 and 5 Hz were chosen. Welding was carried out with filler metals ER1100, ER4043, ER4047 and ER5356. The fillers were chosen based on the work of CAO and KOU [16] who investigated the liquation cracking in the welds of cast A357 alloy. The chemical composition of the as-cast specimen and the filler metals are presented in Table 1. For the present investigation, the current pulsing was used for GTAW of cast A356 alloy. The pulsed current technique has the advantages of controlling the microstructure, reducing grain size and improving the mechanical properties [1, 4, 5, 17]. The welding parameters of GTA welding are presented in Table 2. The photograph of the plates and groove before welding, the macrograph of the real cross section of the weld and the dimension of the groove are shown in Fig. 1.

Table 1 Chemical composition of base metal and fillers used in this work (mass fraction, %)

Element	A356	ER1100	ER4043	ER4047	ER5356
Si	7.15	−	5.2	12	−
Mg	0.32	−	−	−	5
Cu	0.1	0.12	−	−	−
Mn	0.005	−	−	−	0.12
Ti	0.14	−	−	−	0.13
Cr	0.006	−	−	−	0.12
Fe	0.12	−	−	−	−
Zn	0.04	−	−	−	−
Ni	0.007	−	−	−	−
Sr	0.026	−	−	−	−
Al	Bal.	Bal.	Bal.	Bal.	Bal.

The microstructure in the weld bead was studied by the optical and scanning electron microscopes (SEM) equipped with energy dispersive X-ray detector (EDX). It is noted that the samples were prepared from the center of the plate thickness, approximately along the dash point shown in the real cross section. All samples were etched in 5% HF solution for 20 s. Image analysis of micrographs of the weld metal was carried out by image analyzing software (Image Tool).

Table 2 Welding parameters supplied in this work

Process parameter	Value
Electrode	98%W+2%Zr
Electrode size/mm	3.15
Filler metal diameter/mm	2.4
Shielding gas	Argon
Shielding gas flow rate/(L·min^{-1})	18
Welding speed/(cm·min^{-1})	10
Peak current/A	180
Base current/A	70

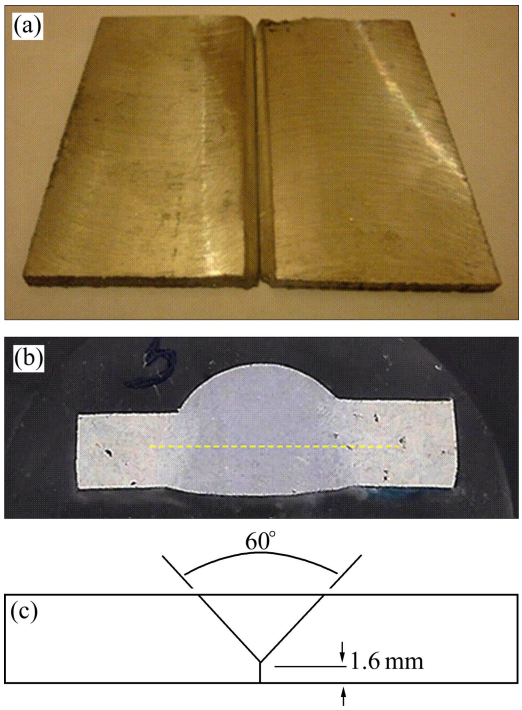

Fig. 1 Photograph of plates and groove before welding (a), macrograph of real cross section of weld (b) and schematic illustration showing dimension of groove (c)

The Vickers microhardness was used for hardness testing. The hardness measurements were taken by applying a load of 100 g for 10 s from the fusion zone to the base metal. Tensile tests were conducted by a computer-controlled universal testing machine with a crosshead speed of 2 mm/min. Impact test was conducted by a Charpy impact test machine. The location and configuration of the specimens used for mechanical testing are shown in Fig. 2.

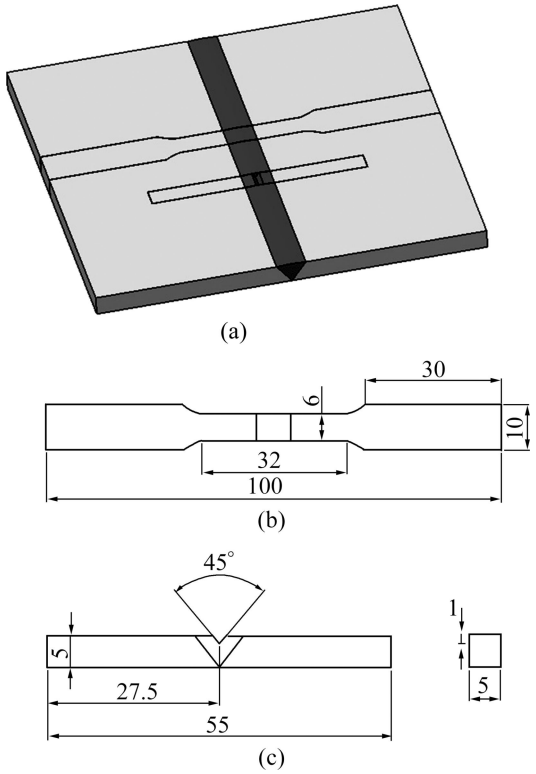

Fig. 2 Schematic illustration of welded plate and location of specimens extracted for mechanical testing (a), and configuration of tensile (b) and impact test specimens (c), respectively (unit: mm)

3 Results and discussion

3.1 Microstructure

The phase behavior of Al−Si system provides a eutectic reaction in which the alloy containing about 12% Si has the eutectic composition. A356 alloy with 7% Si is a hypoeutectic alloy whose Si content is less than the eutectic composition. Therefore, the liquid begins to solidify at the liquidus temperature, producing primary phase α. Solidification is completed after going through the eutectic reaction, leading to a microstructure with a primary phase α and a eutectic structure. The effect of Sr on the size and morphology of eutectic silicon particles is very significant. Strontium changes the morphology of the silicon particles in the unmodified alloy to a fibrous form and also decreases the mean aspect ratio and size of the eutectic particles [18]. In general, the weld bead can be divided into four regions: fusion zone (FZ), partially melted zone (PMZ), heat affected zone (HAZ) and base metal (BM). BM is a part of the specimens whose microstructure is not changed due to the heating effects. The microstructure consists of the coarse dendrite of primary α(Al) and eutectic mixture of Al and Si, which forms between the dendrite arms spacing. Figure 3 shows the micrographs of weld bead covering from FZ to BM after being welded with different fillers.

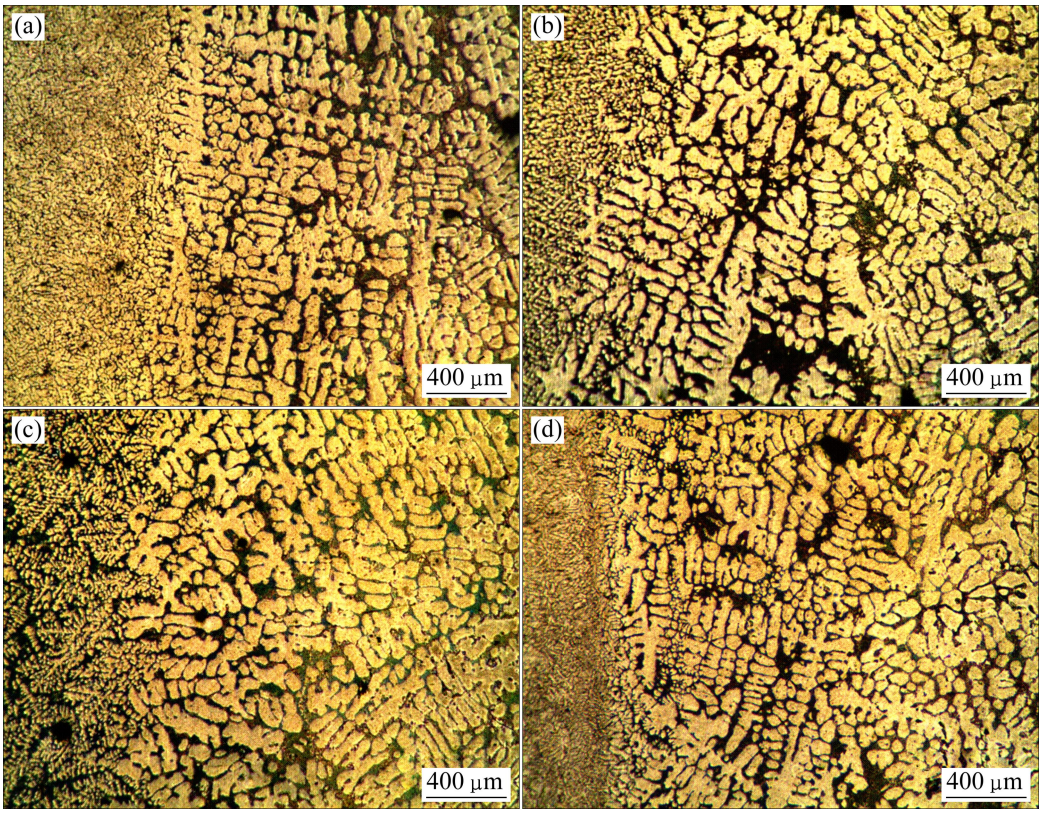

Fig. 3 Micrographs of weld bead under pulse frequency of 3 Hz with filler ER1100 (a), ER4043 (b), ER4047 (c) and ER5356 (d)

All zones consist of a primary α(Al) (bright region) which is a solid solution rich in Al and a eutectic mixture of Al and Si (dark region) that solidifies between the dendrite arm spacing. FZ appears as a fine dendrite structure because of the high cooling rate during solidification. PMZ, HAZ and BM are formed to the right of FZ, respectively. It is observed that the microstructure appearance in PMZ, HAZ and BM is approximately identical for all fillers at the magnification shown in Fig. 3. Nevertheless, the microstructure of the FZ is significantly affected by changing the filler metals. The microstructures of the joint are investigated in detail as explained below. SEM image of the microstructure near the boundary line of the PMZ and HAZ is shown in Fig. 4.

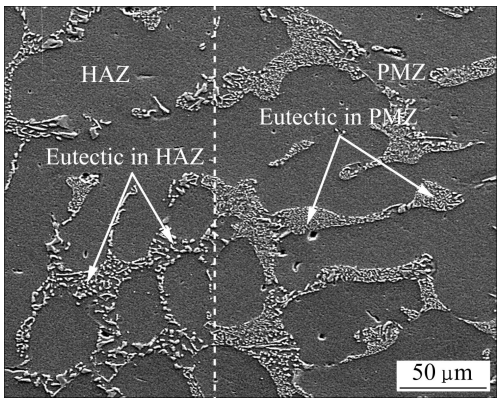

Fig. 4 SEM image of weld (with filler ER4043 under frequency of 3 Hz) near boundary line of PMZ and HAZ

It is seen that the Al−Si eutectic in the HAZ is coarser than that in the PMZ. In addition, Al and Si in the eutectic mixture of the HAZ appear more distinct. This is because, in the HAZ, the alloy is heated to just below the eutectic temperature, causing it to coarsen and separate into the Al matrix and Si particles. The PMZ is a region adjacent to the FZ where the eutectic mixture melts during welding because of heating above the eutectic temperature. The PMZ consists of α dendrites and interdendritic eutectic similar to HAZ. However, contrary to the HAZ, the eutectic structure is finer in PMZ. In other words, Si in the eutectic mixture breaks into somewhat finer particles and disperses more uniformly due to the liquation of the eutectic and rapid solidification rate in PMZ. The microstructural details of the PMZ are presented in Fig. 5. SEM image in Fig. 5 indicates that, in addition to the primary Al and eutectic mixture, another morphologically distinct phase (indicated by arrow) can also be observed. According to the EDX results and the findings published in the literatures [18−20], this phase may be β-phase (Al_5FeSi) intermetallic. The intermetallic phase may be the products of the eutectic reactions whose formation

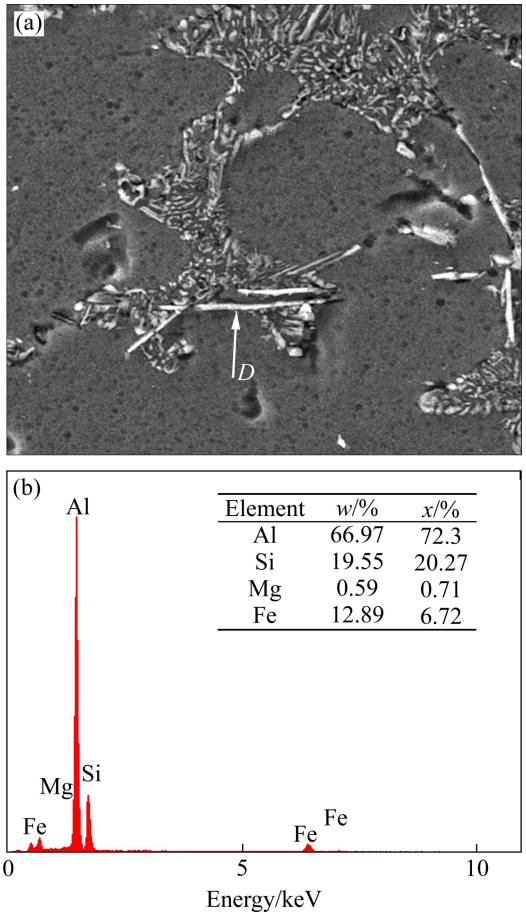

Element	w/%	x/%
Al	66.97	72.3
Si	19.55	20.27
Mg	0.59	0.71
Fe	12.89	6.72

Fig. 5 Typical SEM image in PMZ (a) and EDX analysis corresponding to phase indicated by arrow (b)

depends on the cooling rate and the amounts of each constituting element [15].

Figure 6 shows the optical micrographs of the FZ after being welded with different fillers and frequencies. The microstructure of FZ reveals primary α(Al) formed as dendrites and the interdendritic eutectic mixture. The results show that filler metal and pulse frequency significantly affect the grain structure of FZ. For a given filler metal, the primary α(Al) in the FZ becomes finer and roughly equiaxed when the pulse frequency increases from 1 to 5 Hz. The increase in pulse frequency also causes the decrease in area fraction of eutectic to some extent. In general, the turbulence in the weld pool increases with increasing the pulse frequency. This can promote the fragmentation of the growing dendrites which in turn can lead to the refinement of the grain structure [5]. Figure 6 also reveals that, for a given frequency, the amount of α(Al) dendrites and eutectic mixture is changed for the welds with different filler metals. The volume fractions of the eutectic mixture, determined by the image analyzer software, are 18% for filler ER1100, 35% for filler ER4043 and 44% for filler ER4047. The microstructure of the weld metal is affected by filler metal and BM composition as well as the

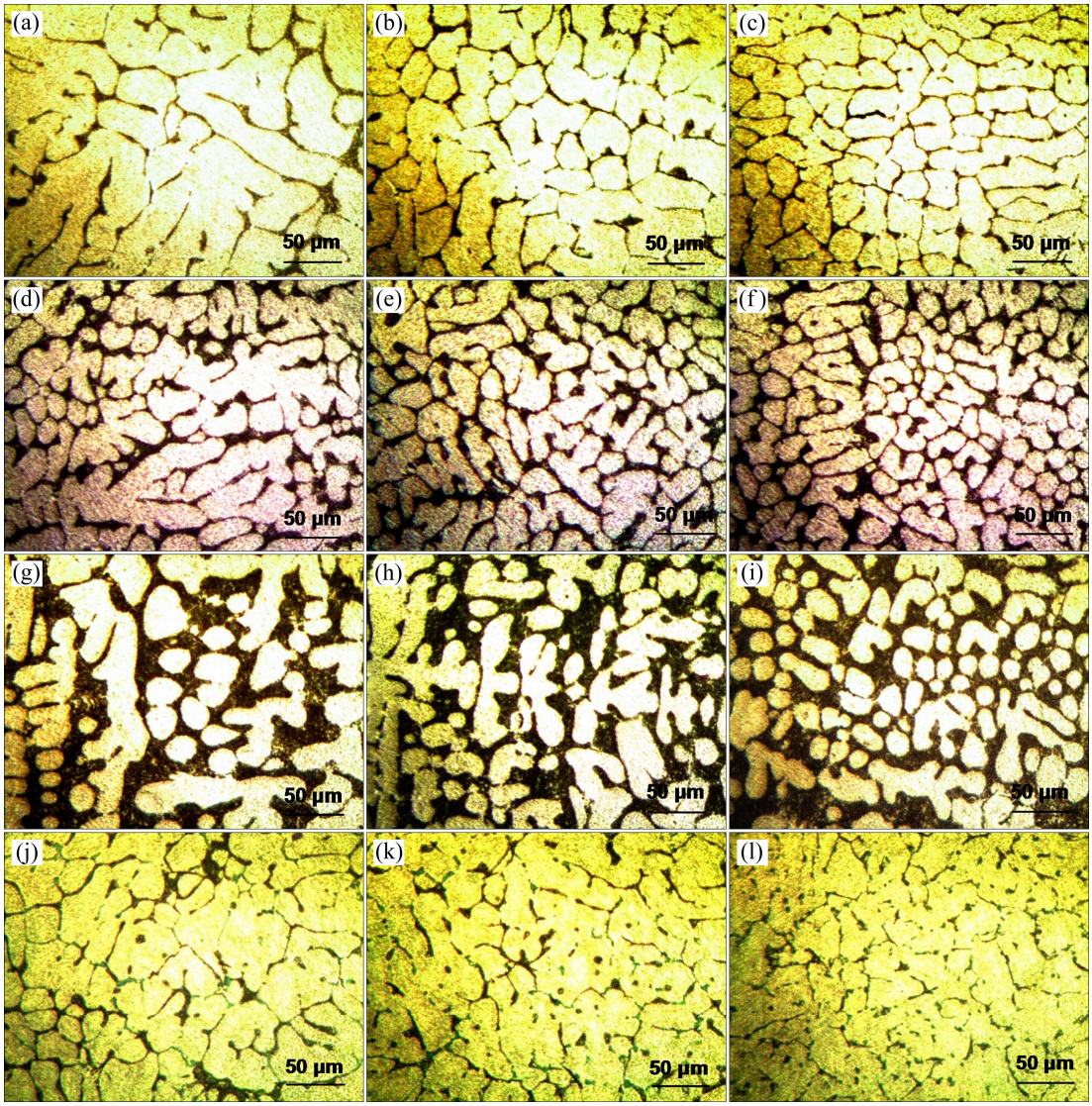

Fig. 6 Optical micrographs in FZ of welds with different fillers under frequency of 1 Hz (a, d, g, j), 3 Hz (b, e, h, k) and 5 Hz (c, f, i, l): (a, b, c) ER1100; (d, e, f) ER4043; (j, h, i) ER4047; (j, k, l) ER5356

dilution ratio. According to lever rule, the fraction of the eutectic mixture increases with increasing the Si content in the FZ.

The highest fraction of eutectic is formed in the welds with the filler ER4047, which has the largest amount of Si. Although, filler ER1100 does not contain any Si element, however, the microstructure of the welds made with this filler shows a small fraction of eutectic mixture. This can be attributed to the slight dilution of the BM into the weld. It is noted that the eutectic constituents in FZ of the welds made with filler ER5356 may be somewhat different because of the Mg content (about 5% Mg). Therefore, SEM image and EDX analysis (Fig. 7) were used to observe the microstructure of these welds at higher magnifications and to analyze the chemical composition of the exhibited points in the microstructure. The results indicate that the composition at the point *A* contains Al and Mg while the composition at point *B* consists of Mg and Si. To identify the type of phases, further structural information is needed.

The effect of pulse frequency on the microstructure of the HAZ is presented in Fig. 8. Contrary to the FZ, it is seen that the pulse frequency does not have any significant effect on the microstructure of the HAZ. This may be attributed to the fact that the heat input for these frequencies is approximately the same, giving no considerable structural change in the HAZ.

3.2 Mechanical properties

The effect of filler metal, pulse frequency and the distance from the weld pool on the hardness is presented in Fig. 9. Generally, for a given filler and frequency, the hardness of the FZ is higher than that of other zones. This is because FZ has a fine dendrite and eutectic structure owing to high cooling rate during solidification.

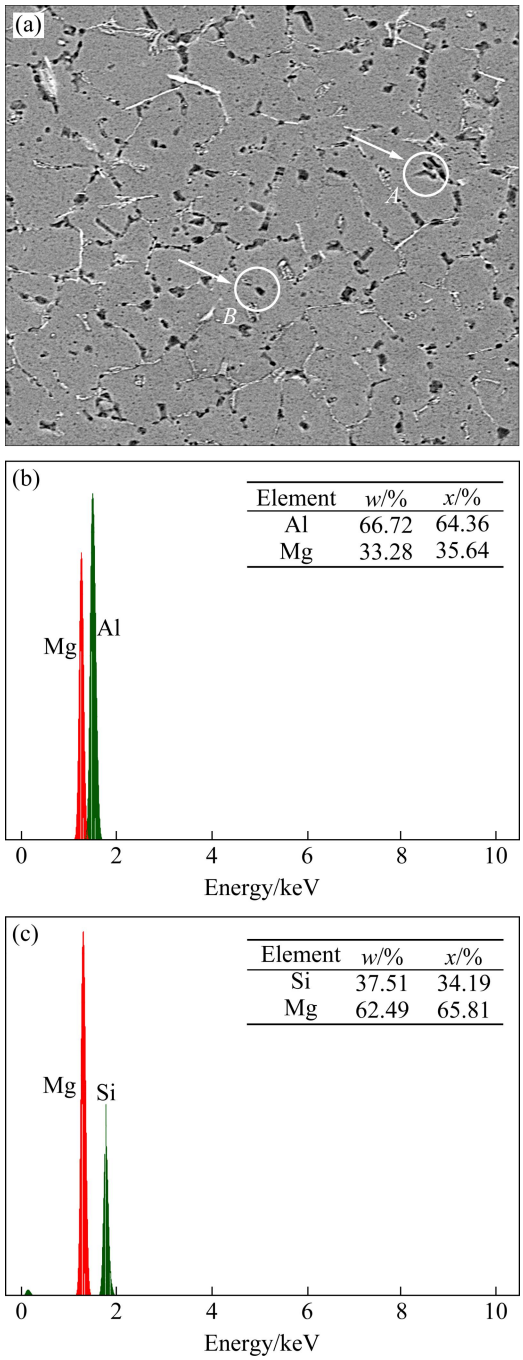

Fig. 7 SEM image in FZ of welds with filler ER5356 under frequency of 3 Hz (a) and EDX analyses corresponding to exhibited points *A* (b) and *B* (c)

It is observed that in the welds with filler ER5356, the hardness in PMZ decreases compared with that of FZ. This may be due to the depletion of the intermetallic precipitates in the PMZ. Conversely, in the welds with fillers ER1100, ER4043 and ER4047, no significant change is observed between the hardness of the FZ and PMZ, particularly at higher frequencies. The lowest hardness is measured in the HAZ (HV 50−60) for all fillers and frequencies due to the heat effects that impose into the HAZ.

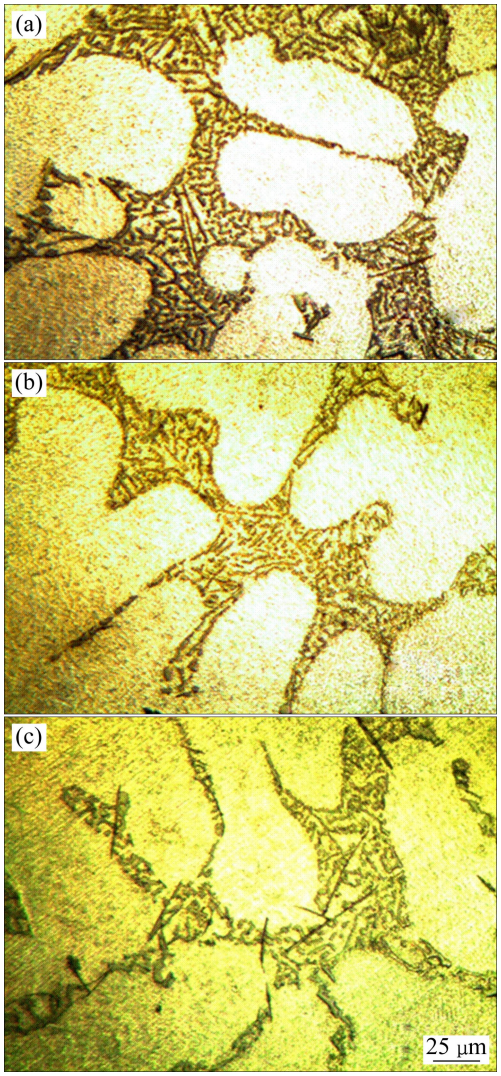

Fig. 8 Optical micrographs in HAZ with filler ER4043 under frequency of 1 Hz (a), 3 Hz (b) and 5 Hz (c)

Generally, the hardness measurements indicate that filler metal can affect the hardness value, particularly in FZ. In this region, the hardness of the welds with filler ER5356 is larger than that of the others, particularly at high frequencies. This can be attributed to the fact that filler ER5356 contains large amount of Mg (about 5%) compared with the other fillers. In general, Mg has a significant effect on the eutectic structure. In addition, the Mg content can remarkably increase the size and volume fraction of the intermetallic. It has been reported that the size and amount of the intermetallic phases depend on the Mg content and the cooling rate during solidification [18,20]. The presence of the intermetallic phases in FZ of the welds with filler ER5356 has been confirmed in the previous sections by SEM/EDX results presented in Fig. 7. These results are consistent with those of HWANG et al [14] where they compared the hardness of the squeeze-cast A356 with fillers ER5356

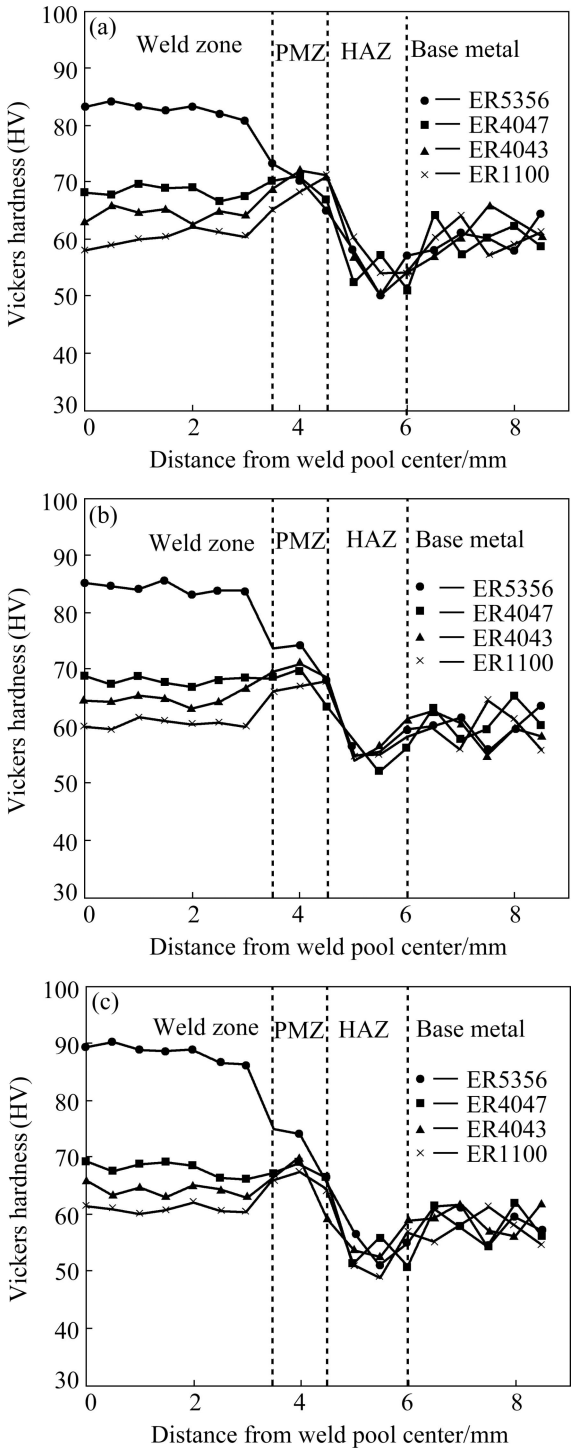

Fig. 9 Microhardness profiles of weld bead with different fillers under frequency of 1 Hz (a), 3 Hz (b) and 5 Hz (c)

and ER4340 under different heat treating conditions.

The hardness results also reveal that among fillers ER1100, ER4043 and ER4047, the largest hardness in FZ is measured for the welds with fillers ER4047 (about HV 70). The difference in the hardness of the welds when using these fillers results from the difference in the fraction of eutectic mixture. Generally, the hardness of the Al/Si eutectic is larger than that of α(Al) because of the Si particles in eutectic. Therefore, the hardness rises with increasing the fraction of the eutectic. The largest fraction of eutectic structure (44%) is formed in the weld with filler ER4047. Accordingly, its hardness is larger than those of the welds with fillers ER1100 and ER4043.

Figure 9 also indicates a large variation in the hardness of the BM while the hardness of the FZ shows more uniform values. It has been pointed out that the hardness of the BM depends on the position of the hardness indenter [7,13], because the α(Al) grain size in BM (about 100 μm) is much larger than the Vickers indenter size. If the indenter is located on the primary α(Al) phase, which is softer than the eutectic mixture, a lower hardness is measured, while when the indenter penetrates into the eutectic, the hardness is higher. Nonetheless, an intermediate value of the hardness is achieved when the indenter is located on both α(Al) dendrites and the eutectic. Hardness measurements also indicate that the pulse frequency does not have a significant effect in the welds that used fillers ER1100, ER4043 and ER4047. However, for the welds with filler ER5356, the effect of pulse frequency is more considerable, particularly in the FZ. For this filler, the hardness of the FZ increases from about HV 82 to about HV 90 when the pulse frequency increases from 1 Hz to 5 Hz.

The effect of filler metal and pulse frequency on the impact toughness is illustrated in Fig. 10. The results show that the weld with filler ER4047 has the largest impact toughness (3−4 J). In general, the impact toughness of the Al/Si eutectic is larger than that of the α(Al) dendrites because of its lamellar structure. The largest volume fraction of eutectic (44%) is formed in welds with filler ER4047, whose Si content is 12%, leading to the highest impact energy. The least amount of impact toughness is observed for the welds with filler ER5356 whose impact toughness is about 1 J for all frequencies. This can be attributed to the formation of the intermetallic phases in the FZ during solidification. It has been reported that pores with greater volume fraction can be produced in the welds with filler ER5356 compared to the welds with filler ER4043. The formation of these pores can also cause the decrease in the impact toughness of the welds [14]. No significant effect of the pulse frequency on the impact toughness is observed in welds with filler ER5356. However, in welds with the fillers ER1100, ER4043 and ER4047, the impact toughness increases slightly with increasing the pulse frequency. This can be attributed to the fact that the microstructure of the welds that utilize higher frequency is finer and more equiaxed, leading to the higher impact energy.

The photograph of the fractured samples after

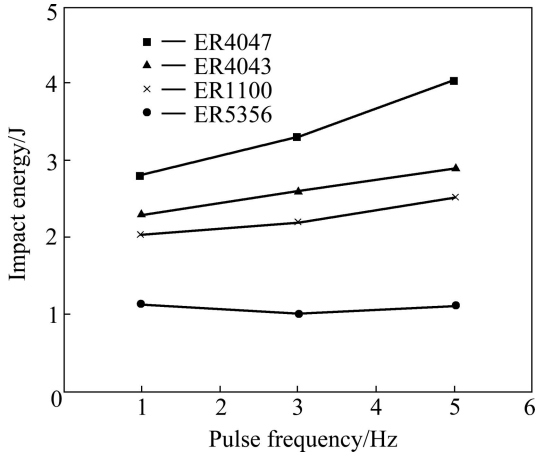

Fig. 10 Variation in impact energy with filler metal and pulse frequency

tensile tests is shown in Fig. 11. It is somewhat difficult to find the weld line from Fig. 11. However, according to the dimension of the groove (Fig. 1), the total groove width is about 4 mm that is 2 mm away from the center of the sample gage length. Considering the total gage length after fracture (about 32 mm) and the approximate position of the centerline (Fig. 11), it can be concluded that fracture must occur in a region other than FZ (more probably in the HAZ). The engineering stress−strain curves of the welds with different fillers and frequencies are presented in Fig. 12. The tensile test results show that the strength and elongation for all specimens are approximately the same, about 120 MPa and 6%, respectively. These results also confirm that the fracture cannot take place in the FZ, because its microstructure is changed with altering the welding conditions (Fig. 6).

Fig. 11 Photograph of tensile test specimens welded under different conditions

It has been shown that the tensile properties of the A356 alloys depend on the size and shape of the silicon particles in the eutectic mixture [21]. Briefly, the mechanism responsible for damage process in A356 alloys includes three stages [18]: particle fracture, microcrack formation, and linkage of microcracks. It has been pointed out that due to the inhomogeneous plastic

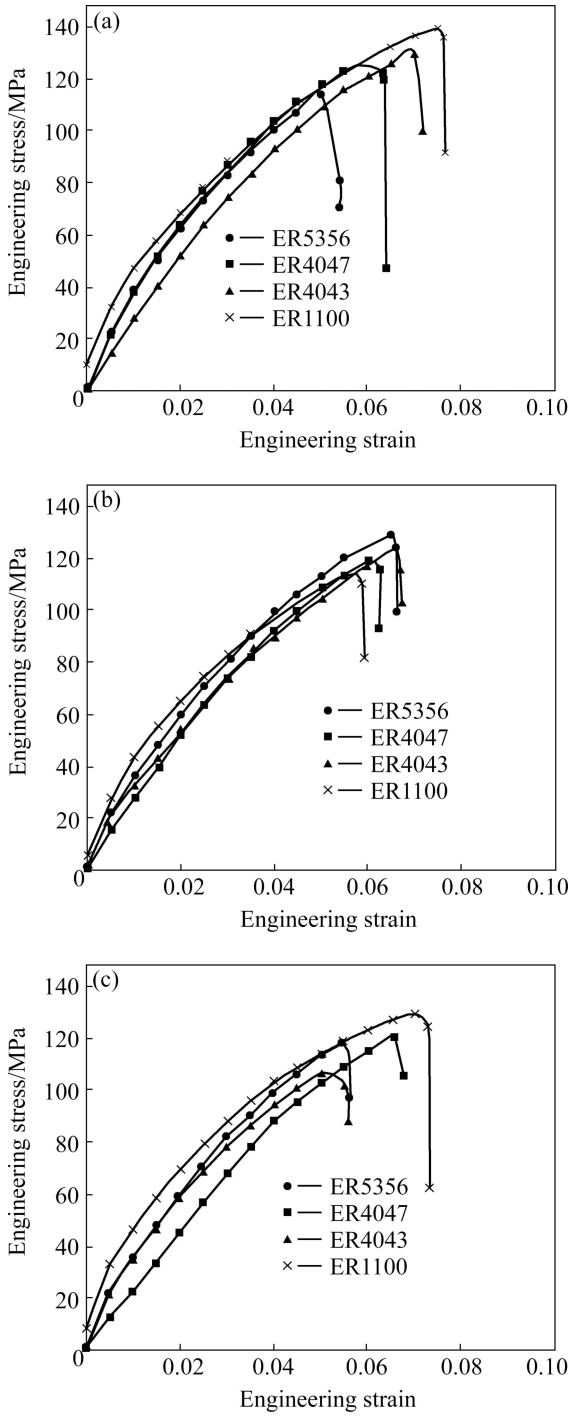

Fig. 12 Typical engineering stress−strain curves of welds with different fillers and frequencies: (a) 1 Hz; (b) 3 Hz; (c) 5 Hz

deformation, the internal stresses can be induced in the eutectic Si particles [22]. When the internal stress developed in the particle reaches the particle fracture strength, the fracture of the particle takes place. In the second stage, the adjacent microcracks join and form larger microcracks. Final fracture of the alloy occurs when the amount of deformation reaches a critical value and the alloy fails by rapid linkage of microcracks. In the presence of casting defects, the tensile fracture of A356

alloy can also be affected by shrinkage defects that originally exist in the BM. These defects act as a location for crack nucleation and growth. Figure 13 illustrates a typical shrinkage defect as well as dendritic arms observed on tensile fracture surface of the weld with filler ER1100.

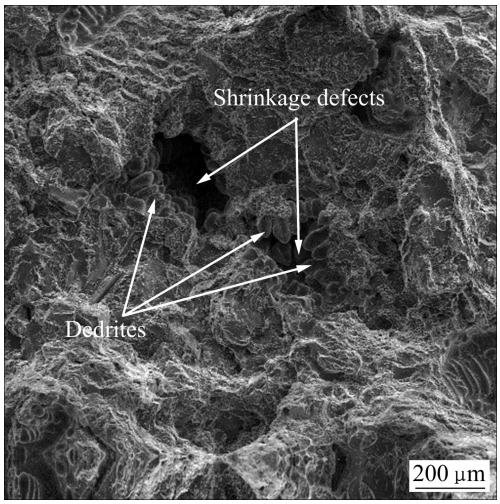

Fig. 13 Typical tensile fracture surface of welded cast A356 alloy with filler ER1100 under frequency of 5 Hz

4 Conclusions

1) The microstructure of the BM consists of coarse dendrite of α(Al) and eutectic mixture. In the HAZ, the eutectic structure coarsens and separates into an Al matrix and Si particles. In the PMZ, Si particles in the eutectic break into somewhat finer particles. Intermetallic phases are formed in the eutectic structure of the PMZ.

2) The FZ appears as a fine dendrite structure. The highest fraction of eutectic in the FZ is formed with filler ER4047 (44%) that has the largest amount of Si. The primary α(Al) in the FZ becomes finer and roughly equiaxed when the pulse frequency increases from 1 to 5 Hz.

3) The lowest hardness is measured in the HAZ (HV 50−60) for all fillers and frequencies due to the heat effects. The hardness of the welds with filler ER5356 is higher than that of the others, particularly in the FZ. The greatest hardness (HV 90) is achieved in the welds with filler ER5356 and pulse frequency of 5 Hz. The welds that use filler ER4047 gives the largest impact toughness (3−4 J). Tensile testing of the welds indicates that fracture does not occur in the FZ.

Acknowledgements

The authors would like to thank the financial support of Shahid Chamran University through the Grant Number EN-636410.

References

[1] KUMAR T S, BALASUBRAMANIAN V, BABU S, SANAVULLAH MY. Effect of pulsed current GTA welding parameters on the fusion zone microstructure of AA 6061 aluminium alloy [J]. Metals and Materials International, 2007, 13: 345−351.

[2] KUMAR A, SUNDARRAJAN S. Effect of welding parameters on mechanical properties and optimization of pulsed TIG welding of Al−Mg−Si alloy [J]. The International Journal of Advanced Manufacturing Technology, 2009, 42: 118−125.

[3] SENTIL KUMAR T, BALASUBRAMANIAN V, SANAVULLAH M Y. Influences of pulsed current tungsten inert gas welding parameters on the tensile properties of AA 6061 aluminium alloy [J]. Materials and Design, 2007, 28: 2080−2092.

[4] MANTI R, DWIVEDI D K, AGARWAL A. Microstructure and hardness of Al−Mg−Si weldments produced by pulse GTA welding [J]. The International Journal of Advanced Manufacturing Technology, 2008, 36: 263−269.

[5] MANTI R, DWIVEDI D K, AGARWAL A. Pulse TIG welding of two Al−Mg−Si alloys [J]. Journal of Materials Engineering and Performance, 2008, 17: 667−673.

[6] SRINIVASA RAO K, PRASAD RAO K. Partially melted zone in Al−Mg−Si alloy gas tungsten arc welds: Effect of techniques and prior thermal temper [J]. Materials Science and Technology, 2005, 21: 995−1002.

[7] LEE W B, YEON Y M, JUNG S B. The improvement of mechanical properties of friction-stir-welded A356 Al alloy [J]. Materials Science and Engineering A, 2003, 355: 154−159.

[8] AMIRIZAD M, KOKABI A H, GHARACHEH M A, SARRAFI R, SHALCHI B, AZIZIEH M. Evaluation of microstructure and mechanical properties in friction stir welded A356+15%SiC_p cast composite [J]. Materials Letters, 2006, 60: 565−568.

[9] JAYARAMAN M, SIVASUBRAMANIAN R, BALASUBRAMANIAN V. Establishing relationship between the base metal properties and friction stir welding process parameters of cast aluminium alloys [J]. Materials and Design, 2010, 31: 4567−4576.

[10] GOSH M, KUMAR K, LAILAS S V, RAY A K. Optimization of friction stir welding parameters for dissimilar aluminum alloys [J]. Materials and Design, 2010, 31: 3033−3037.

[11] HASSAN A S, MAHMOUD T S, MAHMOUD F H, KHALIFA T A. Friction stir welding of dissimilar A319 and A356 aluminium cast alloys [J]. Science and Technology of Welding and Joining, 2010, 15: 414−422.

[12] HABOUDOU A, PEYRE P, VANNES A B, PEIX G. Reduction of porosity content generated during Nd:YAG laser welding of A356 and AA5083 aluminium alloys [J]. Materials Science and Engineering A, 2003, 363: 40−52.

[13] AKHTER R, IVANCHEV L, BURGER H P. Effect of pre/post T6 heat treatment on the mechanical properties of laser welded SSM cast A356 aluminium alloy [J]. Materials Science and Engineering A, 2007, 447: 192−196.

[14] HWANG L R, GUNG C H, SHIH T S. A study on the qualities of GTA-welded squeeze-cast A356 alloy [J]. Journal of Materials Processing and Technololgy, 2001, 116: 101−113.

[15] RATNAKUMAR K, SRINIVASA RAO K. Microstructure and pitting corrosion of partially melted zones of A356 Al−Si alloy welds [J]. Transactions of the Indian Institute of Metals, 2008, 61: 283−291.

[16] CAO G, KOU S. Liquation cracking in full penetration Al−Si welds [J]. Welding Journal, 2005: 63s−71s.

[17] BABU S, KUMAR T S, BALASUBRAMANIAN V. Optimizing pulsed current gas tungsten arc welding parameters of AA6061

aluminium alloy using Hooke and Jeeves algorithm [J]. Transactions of Nonferrous Metals Society of China, 2008, 18(5): 1028−1036.

[18] WANG Q G. Microstructural effects on the tensile and fracture behavior of aluminum casting alloys A356/357 [J]. Metallurgical and Materials Transactions A, 2003, 34: 2887−2899.

[19] CACERES C H, DAVIDSON C J, GRIFFITHS J R, WANG Q G. The effect of Mg on the microstructure and mechanical behavior of Al−Si−Mg casting alloys [J]. Metallurgical and Materials Transactions A, 1999, 30: 2611−2618.

[20] WANG Q G, DAVIDSON C J. Solidification and precipitation behaviour of Al−Si−Mg casting alloys [J]. Journal of Materials Science, 2001, 36: 739−750.

[21] CACERES C H, DAVIDSON C J, GRIFFITHS J R. The deformation and fracture behaviour of an Al−Si−Mg casting alloy [J]. Materials Science and Engineering A, 1995, 197: 171−179.

[22] CACERES C H, GRIFFITHS J R, REINER P. The influence of microstructure on the Bauschinger effect in an Al−Si−Mg casting alloy [J]. Acta Materialia, 1996, 44: 15−23.

气体保护钨极焊接 A356 铸造铝合金的显微组织与力学性能

S. TAKHTI, M. REIHANIAN, A. ASHRAFI

Department of Materials Science and Engineering, Faculty of Engineering, Shahid Chamran University of Ahvaz, Ahvaz 61357−83151, Iran

摘　要：在脉冲频率为 1、3 和 5 Hz 条件下，采用 ER1100、ER4043、ER4047 和 ER5356 焊料对 A356 铸造铝合金进行气体保护钨极焊接，并研究了焊接接头的显微组织和力学性能。研究结果表明，焊料和脉冲频率对熔焊区的晶粒组织有重要影响。采用 ER4047 焊料可得到最高体积分数的共晶组织(44%)。试样的拉伸断口表明断裂并非发生在熔焊区。采用 ER4047 焊料可得到最大的冲击韧性(4 J)，而采用 ER5356 焊料可得到最大的硬度(HV 90)。

关键词：A356 铸造合金；气体保护钨极焊接；显微组织；硬度；冲击能

(Edited by Yun-bin HE)